Effect of heat treatment on thermal diffusivity of Zn/Al layered double hydroxide synthesized using photoflash technique

MARYAM RANJBAR G[a], KAMYAR SHAMELI[b,*], MAHMOOD MAT YUNUS[a], MOHD ZOBIR BIN HUSSEIN[b], KAVEH SHAMELI[c]

[a]*Department of Physics, Faculty of Science, Universiti Putra Malaysia, 43400 Selangor, Malaysia*
[b]*Department of Chemistry, Faculty of Science, Universiti Putra Malaysia, 43400 Selangor, Malaysia*
[c]*Department of Electrical, Electronic and Systems Engineering, Faculty of Engineering and Built Environment Universiti Kebangsaan Malaysia*

Thermal diffusivity of zinc-aluminum layered double hydroxides was synthesized at different molar ratio of zinc and aluminum salts in the pH=7 and measured by using polyvinlidene diflouride (PVDF) by photoflash technique. The samples were prepared using $Zn(NO_3)_2$ and $Al(NO_3)_3$ solutions by drop wise addition of NaOH solution with vigorous stirring under nitrogen atmosphere. The samples then heat treated by control an electrical furnace from 200 to 600 °C for 5 hours. Thermal diffusivity was increased for all samples after sintering. The samples were studied by powder x-ray diffraction method, Fourier transform infrared (FTIR), scanning electron microscope (SEM) and thermal diffusivity. Our results indicate the very different role of sintering in the structure and thermal diffusivity of samples.

(Received November 3, 2013; accepted May 15, 2014)

Keywords: Thermal diffusivity, Zn/Al Layered Double Hydroxide, Photoflash, Polyvinlidene diflouride, Heat treatment

1. Introduction

Thermal diffusivity is a basic thermal property of materials and its accurate value is often needed in many branches of physics and chemistry. Although numerous methods for measuring the thermal diffusivity of solid samples were reported but the photothermal technique was found to be the easiest and simplest method for determining thermal diffusivity of solid samples [1–2].

Inorganic–organic nanocomposite materials with functional organic compounds immobilized into a layered inorganic matrix have potential to offer scientific and technological advantages, since the organized two-dimensional arrays of organic species between the interlayers can result in novel functions that are different to the typical functions of the individual organic species [3–11].

An electrostatic layer-by-layer assembly technique that employs inorganic nanocomposites as building blocks is a possible means of forming a well-ordered multilayered architecture containing the arrays, because the nanocomposites have ultimate two-dimensional anisotropy with nanoscale thickness and microscale length in the plane of sheet [12]. It is known that some smectite clay minerals like montmorillonite, metal phosphates and layered oxides can be exfoliated into negatively charged nanosheets [13]. In contrast, positively charged nanosheets are a minority among exfoliated nanosheets. Recently, the exfoliation of layered double hydroxides (LDHs) has been studied as a method of preparing such positively charged nanosheets [14]. LDH nanosheets have high potential for use as building blocks to integrate negatively charged organic molecules into restricted arrays, due to their high stability and compatibility with many functional molecules [15–18].

The aim of this paper is to report the change on structure of Zn/Al layered double hydroxide (LDH) by using XRD, FTIR and SEM and also change on thermal diffusivity of Zn/Al-LDH by using a simple polyvinlidene difluoride (PVDF) photothermal technique after heat–treating from 200 to 600 °C. The Zn/Al-LDH sample was chosen because it has many applications, such as flame retardant that can be used to enhance the properties of polymers. It is reported that LDHs to the flame retardancy of the polymeric matrix, producing a refractory oxide residue on the surface of the material and releasing aqueous vapor and carbon dioxide during the decomposition. The endothermic nature of these processes and the dilution of combustible gases of pyrolysis increase the ignition time and reduce the heat release during the combustion [19–21]. In the present measurement, LDH samples were prepared at ratio four of Zn/Al for pH=7 and then heated at 200, 400 and 600 °C, then studied the effect of heat treatment on structure and thermal diffusivity.

2. Experimental section

A schematic diagram of the experimental setup is presented in Fig. 1. The system consists of a photoflash as

a heating source and a film as a sensitive photothermal sensor. Avulcanized rubber was used as a backing material, and the sample was attached to the PVDF film using a thin layer of grease. The PVDF film thickness was 52 μm with the dimension of (12×30) mm^2. The photoflash was fixed at a position 3 cm from the sample surface and pulse duration was 5 ms. The photo-thermal signal was captured using a digital oscilloscope (Le Croy 9310A) equipped with averaging facilities. The experimental data was then plotted using software where the fitting procedure has been carried out based on the squared pulse approximation [22].

The sample with pH=7 and ratio (R) = 4 of Zn/Al-LDH was synthesized by spontaneous self-assembly method of mixed aqueous solutions of $Zn(NO_3)_2$ and $Al(NO_3)_3$. The pH value was controlled by dropwise additions of NaOH solution under nitrogen atmosphere. The precipitate formed was aged at 70 °C in an oil bath shaker for 18 hours. The solution was then centrifuged and washed several times with decarbonated water and dried in an oven at 70 °C for 48 hours [23–25]. The sample was grounded into fine powder and pressed to be a pellet form with 1.3 cm diameters and 0.75 mm thickness using a hydraulic pressing machine (Cover model 4350.L) for 10 minutes. After that sample was heat treated at 200, 400 and 600 °C by an electric furnace (Vulcan 3-130) at atmospheric pressure for 5 hours at a rate of 5 °C/min for future measuring of thermal diffusivity in room temperature.

A Shimadzu XRD 6000 diffractometer with nickel filtered Cu-Kα (λ = 0.1542 nm) beam operated at 30 kV and 30 mA was used to determine the spacing of the Zn-Al-LDH, and ZnO composites using Bragg's equation $n\lambda = 2dsin\theta$. Data were recorded in 2θ range of 2º–60º using the scan rate of 2 º/min.

The scanning electron micrographs of tensile fracture surface of the samples were recorded by a JSM-6400 scanning microscope which is a state-of-the-art high resolution scanning electron microscope with a modern digital image processing system. This SEM Joel operated at 20 kV to investigate the surface morphology of samples. The samples were coated with gold by a Bio-rad coating system before viewing. The scanning electron micrographs were recorded at the magnification of 2600X.

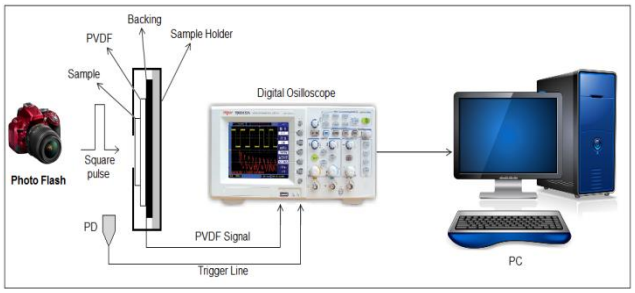

Fig. 1. The schematic diagram of the experimental setup.

3. Results and discussion

Fig. 2 shows the X-ray diffraction patterns obtained for samples prepared at pH = 7 for ratio R=4. As shown in Fig 2, the peaks appear around 30°<2θ< 37° are due to ZnO peaks. The ZnO peaks for pH 7 are increase by increasing the sintering temperature from 200 to 600 °C and the highest ZnO peaks is belong to sample sinter at 600 °C. That is due to reactions crystallinity were completed and with the increase temperature the structure of ZnO completed.

All the diffraction peaks are well indexed to the hexagonal ZnO wurtzite structure (JCPDS no. 36–1451). The diffraction peaks corresponding to the impurity were not found in the XRD patterns. The average particle size of ZnO can be calculated using the Debye-Scherrer Equation (1).

$$n = \frac{K\lambda}{\beta \cos\theta} \quad (1)$$

Where K is the Scherrer constant with value from 0.89 to 1.0 (shape factor), where λ is X-ray wavelength (1.5418 Å), $\beta_{1/2}$ is the width of the XRD peak at half height and θ is the Bragg angle. From the Scherrer equation the average crystallite size of ZnO for samples are found to be lower than 47 nm in size.

Also can be seen two peaks at around 2θ= 10° and 2θ= 20° that are belong to LDH. It can be clearly shown that the LDH peak decreased for the sample with heat treatment at 200 °C. And then the LDH peak for the sample heated at 400 °C is disappeared completely and for also for the sample heated at 600 °C as well.

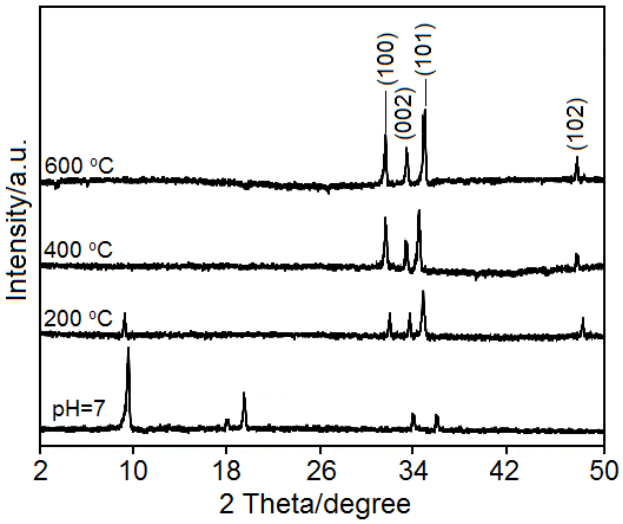

Fig. 2. The X-ray diffraction pattern after different furnace temperatures of 200–600 °C.

Thermal diffusivity of zinc-aluminum layered double hydroxide was studied for the samples at pH 7 and ratio

R = 4 with different sintering temperature from 200 °C to 600˚C.

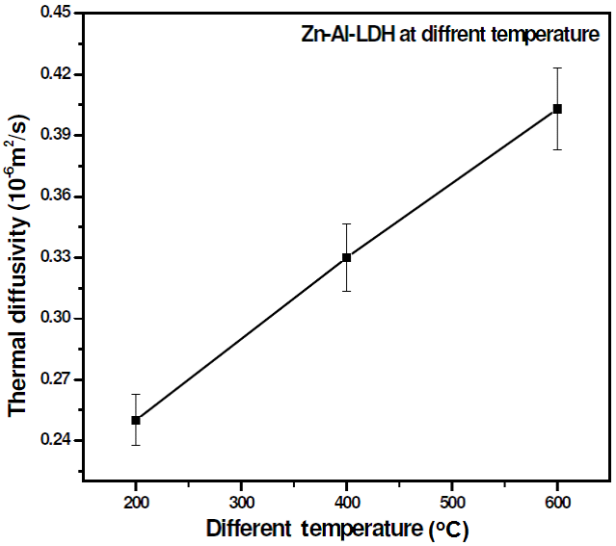

Fig. 3. Thermal diffusivity versus furnace temperatures of 200°–600° C.

As shown in Fig. 3, thermal diffusivity of Zn/Al-LDH for pH 7 increased with increase of sintering temperature from 200 to 600 °C. Thermal diffusivity for sample at pH 7, ratio R = 4 after sintering at 200 ˚C was obtained at 0.25 ± 0.05 $10^{-6}\,m^2\,/s$ and then increase to 0.33 ± 0.06 $10^{-6}\,m^2\,/s$ and 0.40 ± 0.06 $10^{-6}\,m^2\,/s$ for the sample sinter at 400 and 600 °C respectively.

All values of thermal diffusivity for different sintering temperature were summarized in Table 1 in the following:

Table 1. Effect of different heat treatments in values of thermal diffusivity.

Temperature	Thermal diffusivity $10^{-6}m^2\,/\,s$
200 °C	0.25 ± 0.05
400 °C	0.33 ± 0.06
600 °C	0.40 ± 0.06

The FTIR spectrum of the sample at pH 7, ratio R = 4 is shown in Fig 4. A broad band at 3438 cm^{-1} is due to the O−H stretching due to the presence of hydroxyl groups and physically adsorbed water molecule [26]. There is a strong sharp peak at 1384 cm^{-1} due to ν^3 vibrational model of NO_3^- with D_{3h} symmetry, the counter anion in the Zn/Al-LDH, the counter anion in the Zn/Al–LDH.

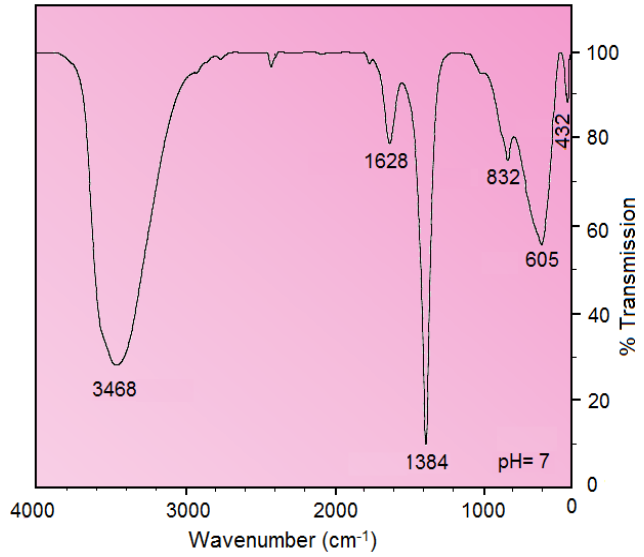

Fig. 4. FTIR spectra the samples prepared at pH 7, at ratio 4.

A weak peak at around 832 cm^{-1} is also present and this reflects the ν_2 mode of the same anion [27]. The band at 1628 cm^{-1} is due to δ H–O–H bending vibration. The Band at 605 cm^{-1} is due to the δ-mode of the O–H groups. The band at 431cm^{-1} is attributed to the Zn–OH and Zn–O lattice vibrations [28].

The FTIR spectrum of the heat-treated sample at 400 °C and 600 °C are shown in Fig. 5 and 6. A broad band at 3438 cm^{-1} is due to the O−H stretching due to the presence of hydroxyl groups and physically adsorbed water molecule. The high intensity band at 1384 cm^{-1} is attributed to the ν^3 nitrate group. A band at 1630 cm^{-1} can be associated to δ-mode of the O−H groups. A band at 1024 cm^{-1} is attributed to the activated ν_1 mode of D_{3h} [29].

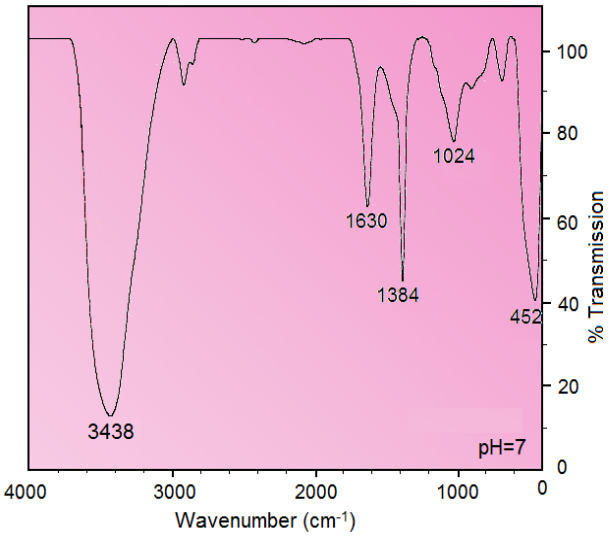

Fig. 5. FTIR spectra the samples prepared at pH 7 after calcined at 400 °C in a furnace.

Although there is no peak associated with a layered structure material in its PXRD pattern, it can be considered that the band at 1384 cm^{-1} is due to the ν_3 nitrate group. This is because the nitrogen group is decomposed completely at temperatures as high as 400°C though the dehydroxylation process is completed at lower temperature (200 °C) [30]. Moreover, the band at 1384 cm^{-1} implies that most retained nitrogen anions are still intercalated in stable state, despite the completion of dehydroxylation for this sample [27]. But a band at 1024 cm^{-1} shows that the sample contains little amount of monodentate nitrate group too. This is because nitrogen anion can attach to the metal cation during dehydroxylation and from an intermediate species M–O...NO_2. The bands at 452 cm-1 show Zn–O lattice vibrations.

With the lowering or disappearing of intensities for the hydroxyl groups and interlayer anions, NO^-_3 for the calcined samples (200–600 °C), the Zn–O vibrational absorption has increased obviously [28]. As shown in Fig. 5 and 6, the intense peaks around 3468 cm^{-1} and 691 cm^{-1} are sharper than pH 7 but the peaks that indicating NO^-_3, around 1384 cm^{-1} very weak comparable to at pH=7. Also a strong broad absorption band at around 691 cm^{-1} indicating the presence of Zn–O and Al–O.

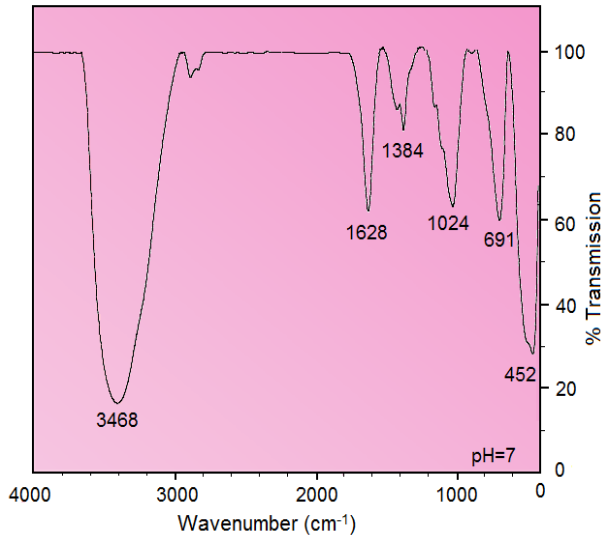

Fig. 6. FTIR spectra the samples prepared at pH 7 after calcined at 600 °C in a furnace.

The scanning electron micrograph of the sample before sintering and after sintering at 600 °C was shown in Fig. 7. As shown in Fig. 7 (a–b), the amorphous structure shape of Zn/Al-LDH prepared at pH 7 in Fig. 7a change to the crystal structure form in Fig. 7b.

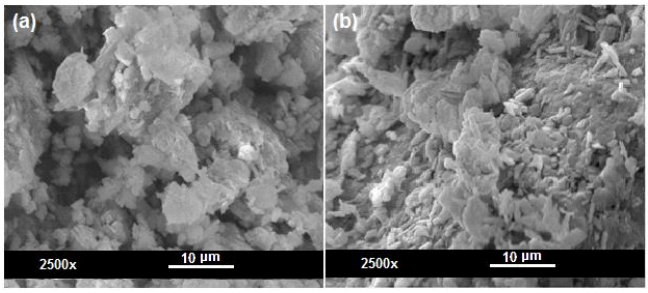

Fig. 7. Surface morphology of Zn/Al-LDH prepared at pH 7 before and after sintering at 600 °C (a–b).

4. Conclusions

Samples of Zn-Al-LDH for pH = 7, R = 4 have been prepared and then were sintered from 200 to 600 °C to measure thermal diffusivity in room temperature. All samples were investigated by XRD, SEM and FTIR. The pH and the sintering temperature of sample with pH 7 and ratio 4 are the important parameters to control the thermal diffusivity of the LDH sample. Thermal diffusivity of Zn/Al-LDH prepared at pH 7 was increased with increasing of sintering temperature from 200 to 600 °C. The highest thermal diffusivity was found for sample with 600 °C and at about 0.40 $10^{-6} m^2 / s$.

Acknowledgements

The authors gratefully acknowledge the department of physics, UPM for providing the research facilities to enable us to carry out this research. They are also grateful to the staff of the department of physics UPM for the technical assistance.

References

[1] M. Haydari, M. M. Moksin, W. M. M. Yunus, I. V. Grozescu, I. Hamadneh, S. A. Halim, Proceddings of SPIE **5581,** 315 (2004).
[2] R. E. Imhof, D. J. S. Birch, F. R. Thornley, J. R. Gilchrist, T. A. Strivens, J. Phys. E **17,** 512 (1984).
[3] M. Eili, K. Shameli, N. A. Ibrahim, W. M. Z. Wan Yunus. Int. J. Mol. Sci. **13**, 7938 (2012).
[4] M. B. Ahmad, K. Shameli, W. M. Z. W. Wan Yunus, N. A. Ibrahim. Aust. J. Basic. Appl. Sci. **7**, 2158 (2010).
[5] M. B. Ahmad, K. Shameli, W. M. Z. W. Wan Yunus, N. A. Ibrahim. Am. J. Appl. Sci. **11**, 1909 (2009).
[6] M. B. Ahmad, M. Y. Tay, K. Shameli, M. Z. Hussein, J. J. Lim. Int. J. Mol. Sci. **12**, 4872 (2011).
[7] K. Shameli, M. B. Ahmad, S. D. Jazayeri, P. Shabanzadeh, P. Sangpour, H. Jahangirian. Chem. Cent. J. **6**, 1 (2012).
[8] K. Shameli, M. B. Ahmad, E. A. Jaffar Al-Mulla, N. A. Ibrahim, P. Shabanzadeh, Molecules **17**, 8506 (2012).

[9] K. Shameli, M. B. Ahmad, S. D. Jazayeri, P. Shabanzadeh. Int. J. Mol. Sci. **13**, 6639 (2012).
[10] K. Shameli, M. B. Ahmad, A. Zamanian, P. Sangpour, P. Shabanzadeh, Y. Abdollahi, M. Zargar. Int. J. Nanomed. **7**, 5603 (2012).
[11] M. B. Ahmad, J. J. Lim, K. Shameli, N. A. Ibrahim, M. Y. Tay. Molecules **16**, 7237 (2011).
[12] S. Srivastava, N. A. Kotov. Acc. Chem. Res. **41**, 1831 (2008).
[13] S. J. Ahmad, Y. D. Li. W. Huang. J. Mater. Sci. **39**, 1919 (2004).
[14] T. Hibino, W. Jones. J. Mater. Chem. **11**, 1321 (2001).
[15] P. Shabanzadeh, N. Senu, K. Shameli, F. Ismail, M. Mohaghegh Tabar. Dig. J. Nanomater. Bios. **8(2)** 541 (2013).
[16] K. Shameli, M. B. Ahmad, S. A. Khorramie, R. Lotfi, A. Zamanian, P. Shabanzadeh, Dig. J. Nanomater. Bios. **8(3)** 981(2013).
[17] S. A. Khorrami, M. B. Ahmad, R. Lotfi, K. Shameli, S. Sedaghat, P. Shabanzadeh, M. A. Baghchesara, Dig. J. Nanomater. Bios. **7(3)** 871 (2012).
[18] H. Hariharan, N. A. AL-Harbi, P. Karuppiah, S. K. Rajaram. Chalcogenide Lett. **9(12)** 509 (2012).
[19] M. Z. Hussein, T. K. Hwa, J. Nanopart. Res. **2,** 293 (2000).
[20] M. Z. Hussein, Z. Zainal, A. H. Yahya, D. W. V. Foo, J. Control. Release **82,** 417 (2002).
[21] M. Z. Hussein, A. H. Yahya, M. Shamsual, H. M. Salleh, T. Yap, J. Kiu, Mater. Lett. **58,** 329 (2004).
[22] M. Haydari, M. M. Moksin, W. M. M. Yunus, V. I. Grozescu, Z. A. Wahab, B. Z. Azmi, Nondestructive Testing and Evaluation **23,** 163 (2008).
[23] E. Ruffio, D. Saury, D. Petit, Int. J. heat Mass Tran. **64,** 1064 (2013).
[24] S. V. Trukhanov, V. V. Fedotova, A. V. Trukhanov, S. G. Stepin, H. Szymczak, Crystallogr. Rep. **53,** 1177 (2008).
[25] S. V. Trukhanov, A. V. Trukhanov, S. G. Stepin, H. Szymczak, C. E. Botez, Fiz. Tverd. Tela. **50,** 886 (2008).
[26] C. Liang, Y. Shimizu, M. Masuda, T. Sasaki, N. Koshizaki, Chem. Mat. **16,** 963 (2004).
[27] Z. P. Xu, H. C. Zeng, Chem. Mat. **12,** 3459 (2000).
[28] F. Billes, M. I. Ziegler, P. Bombicz, Vib. Spectroscopy, **43,** 193 (2007).
[29] N. Zotov, K. Petrov, M. Dimitova-Pankova, J. Phys. Chem. Solids **51,** 1199 (1990).
[30] S. Aisawa, H. Kudo, T. Hoshi, S. Takahashi, H. Hirahara, Y. Umetsu, E. Narita, J. Phys. Chem. Solids. **177,** 3987 (2004).

*Corresponding author: kamyarshameli@gmail.com